Supplemental Information

Activity-Induced Regulation of Synaptic Strength through the Chromatin Reader L3mbtl1

Wenjie Mao, Anna C. Salzberg, Motokazu Uchigashima, Yuto Hasegawa, Hanno Hock, Masahiko Watanabe, Schahram Akbarian, Yuka Imamura Kawasawa, and Kensuke Futai

SUPPLEMENTAL INFORMATION

SUPPLEMENTAL FIGURES

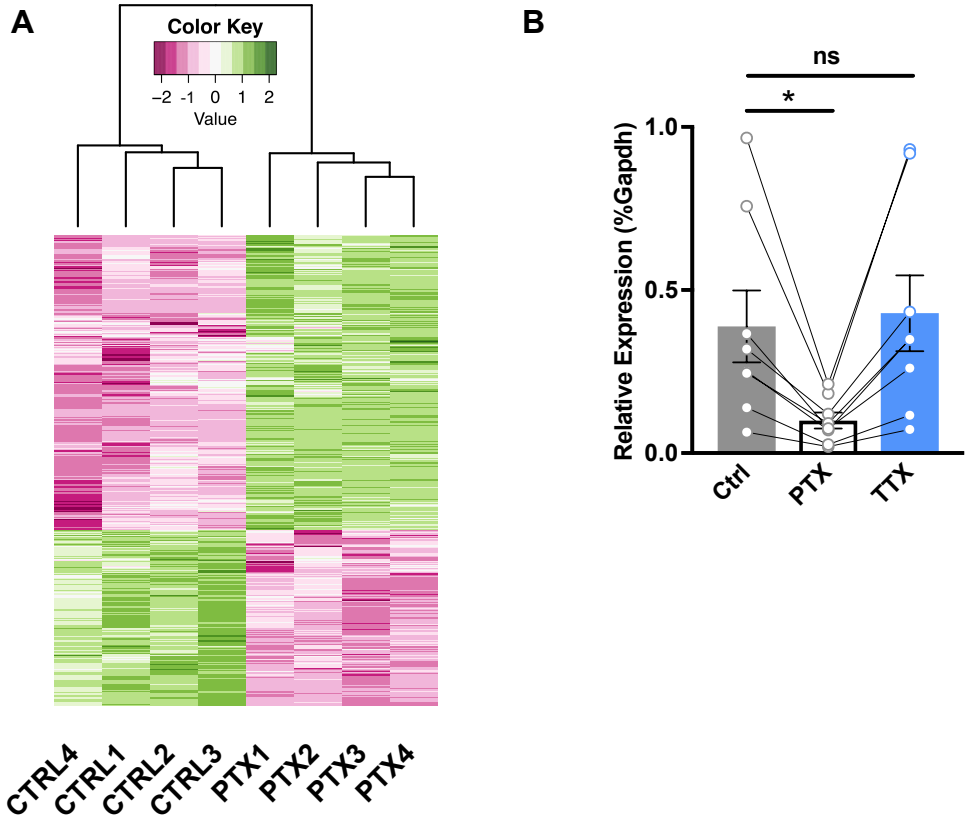

Figure S1. Heat map of activity-dependent gene expression and the validation of activity-dependent expression of L3mbtl1. Related to Figure 1A-B. (A) Heat map of 1839 significant genes by RNAseq analysis from control and PTX-treated hippocampal primary neurons. $p<0.01$ and fold change>2.0 were applied to determine significant differences between control (CTRL1 to 4) and PTX-treated (PTX1 to 4) groups. Hierarchical clustering tree of the samples is shown at the top of the figure. **(B)** Activity elevation but not suppression changed the expression of L3mbtl1. Activity blockade by TTX (1 µM) did not induce a change in expression in primary cultures. Data shown are means ± SEM. * $p=0.026$, one-way ANOVA followed by Sidak's multiple comparisons test, N = 8. Connecting lines indicate matched samples from the same batch.

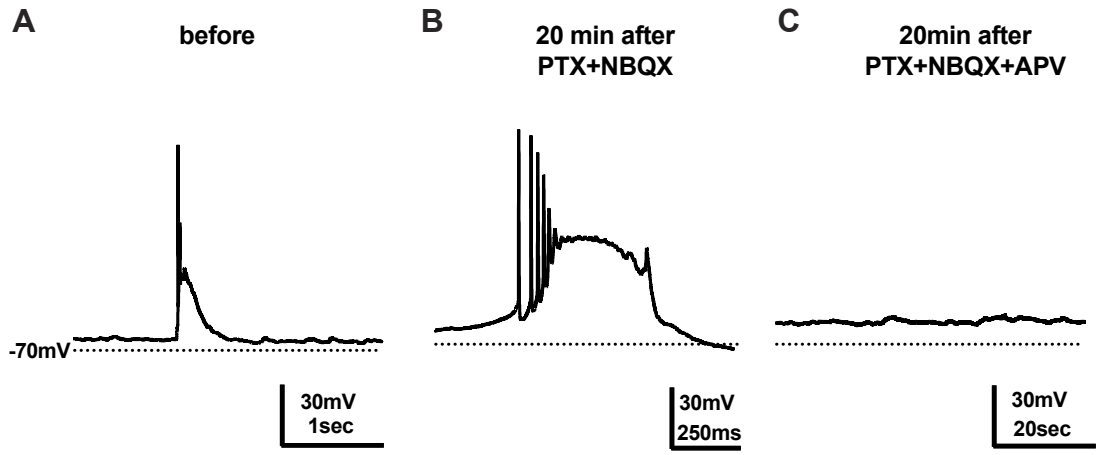

Figure S2. NMDAR activation causes epileptiform bursts in primary neurons. Related to Figure 1H.
Current-clamp recordings were performed from DIV14 hippocampal primary neurons prepared from wild type mice. Representative traces from the same neuron obtained before drug application (A), 20 min after PTX+NBQX (B), and 20 min after PTX+NBQX+APV treatments (C). The spiking frequency of each condition: (A) 0.363 ± 0.054 Hz, (B) 0.028 ± 0.004 Hz, and (C) 0 Hz, N=3.

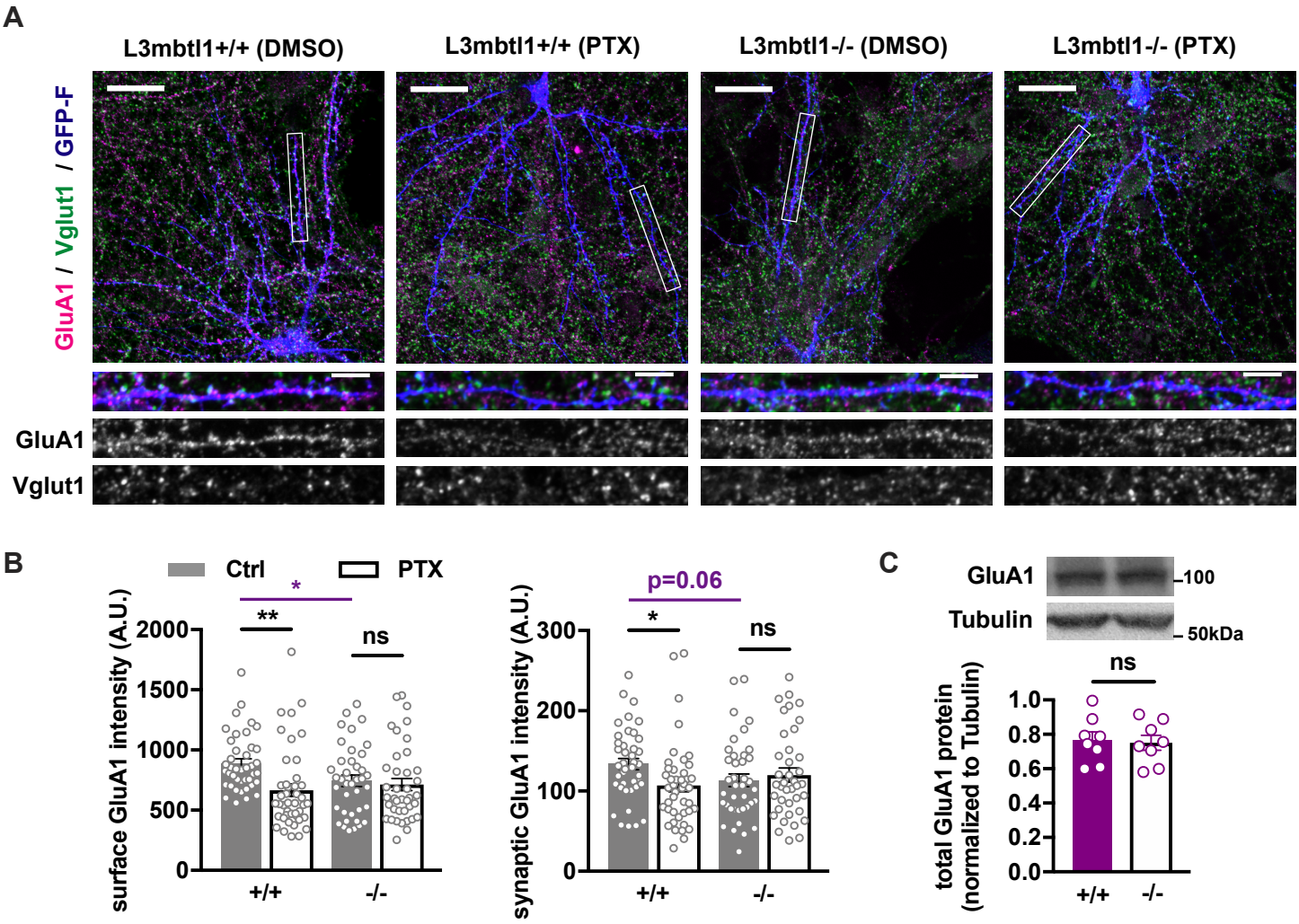

Figure S3. L3mbtl1 is required for homeostatic down-scaling of GluA1-containing AMPA receptors in hippocampal primary neurons. Related to Figure 2. (A-B) Hippocampal primary cultures were prepared from wild type (L3mbtl1 +/+) or L3mbtl1 KO (L3mbtl1 -/-) mice. Neurons were transfected with EGFP-F and treated with PTX (100 µM) or DMSO as control for 48 hrs, fixed and stained for endogenous surface GluA1 and the presynaptic marker Vglut1. **(A)** Representative images of EGFP-F (blue), surface GluA1 (magenta) and Vglut1 (green) immunostaining at low magnification (top; scale bar: 20 µm) and high magnification (bottom; scale bar: 5 µm). **(B)** Quantification of surface GluA1 intensity (left) and Vglut1-colocalized synaptic GluA1 intensity (right) per 20 µm dendritic length in arbitrary units. 39-43 neurons from 8 mice were analyzed for each condition. **p<0.01, *p<0.05, ns: not significant. Student's t-test was performed between wild type and KO control groups (purple indicators); all other comparisons were two-way ANOVA with Sidak's multiple comparisons test. **(C)** Total GluA1 levels in wildtype and L3mbtl1 KO neurons. Representative immunoblots of GluA1 and tubulin (top) and quantification (bottom) of total GluA1 protein in primary cultures prepared from wildtype (+/+) and L3mbtl1 KO (-/-) mice. ns, not significant, student's t-test, N = 8 independent culture batches. Data shown are means ± SEM.

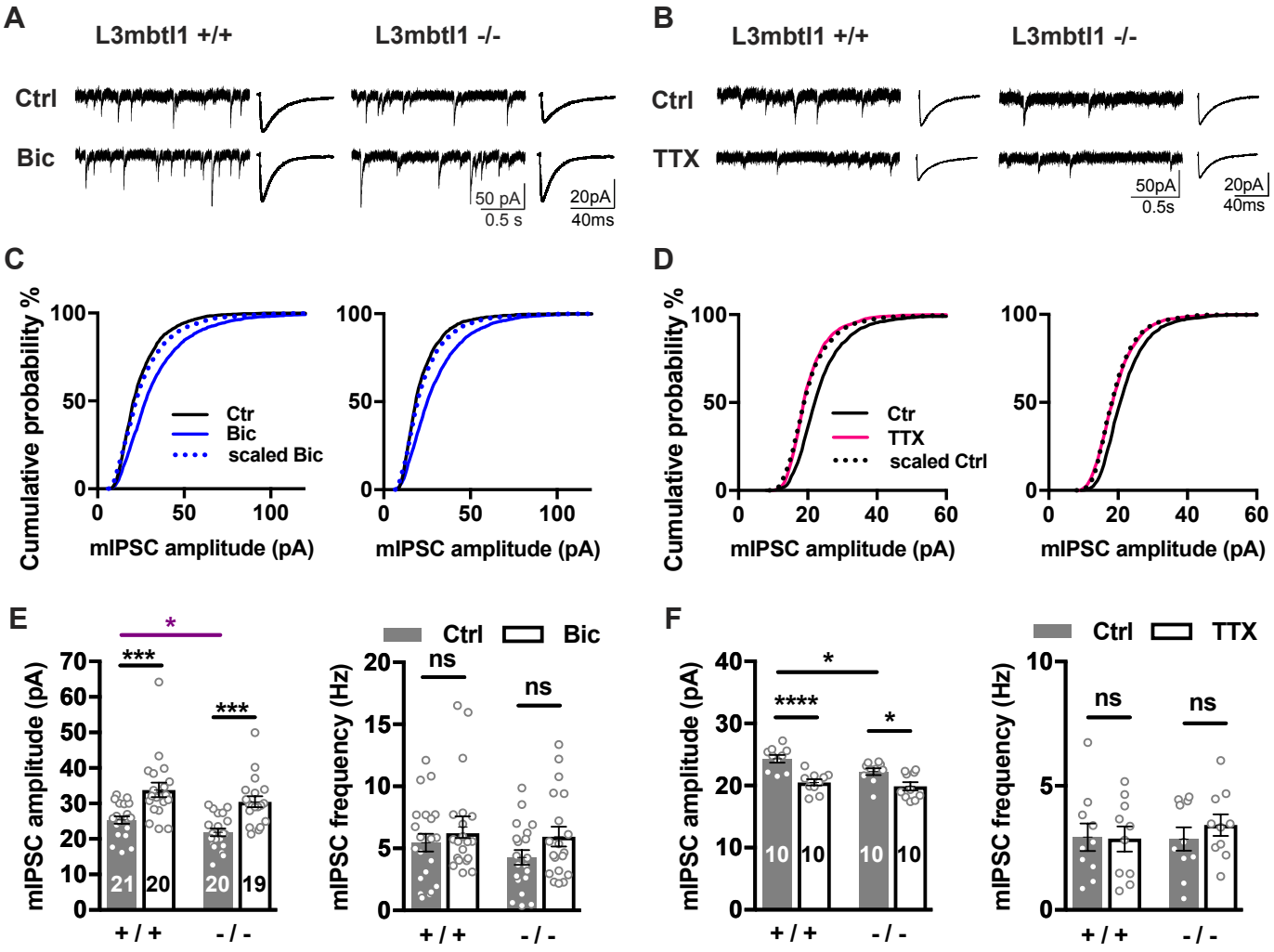

Figure S4. L3mbtl1 is not required for homeostatic up-scaling and down-scaling in inhibitory synapses. Related to Figure 2. Hippocampal primary cultures were treated with Bicuculline (100 μM) to induce up-scaling (A, C, E) or TTX (1 μM) to induce down-scaling (B, D, F). Amplitudes and frequencies of mIPSCs were measured after 48hrs of treatment from wild type (L3mbtl1 +/+) or L3mbtl1 KO (L3mbtl1 -/-) neurons. DMSO treatment was used as control. **(A, B)** Representative mIPSC traces (left) and average mIPSC event traces (right). **(C, D)** Cumulative distribution of mIPSC amplitudes. Scaled distributions were plotted by multiplying the distribution by a scaling factor and removing values that fell below the detection threshold. KS tests for wild type distributions: Ctrl vs Bic, $p=1.6 \times 10^{-46}$; Ctrl vs scaled Bic, not significant; Ctrl vs TTX, $p=9.3 \times 10^{-53}$; scaled Ctrl vs TTX, not significant. KS tests for KO distributions: Ctrl vs Bic, $p=7.6 \times 10^{-51}$; Ctrl vs scaled Bic, not significant; Ctrl vs TTX, $p=2.0 \times 10^{-31}$; scaled Ctrl vs TTX, not significant. **(E, F)** Quantification of mean mIPSC amplitudes (left) and frequencies (right). Data shown are means ± SEM. ****p<0.0001, ***p<0.001, *p<0.05, ns, not significant. Student's t-test was performed between wild type and knockout control groups in E (purple asterisk); all other comparisons were two-way ANOVA with Sidak's multiple comparisons test. N = 6 - 7 mice were tested for up-scaling; N = 4 mice were tested for down-scaling.

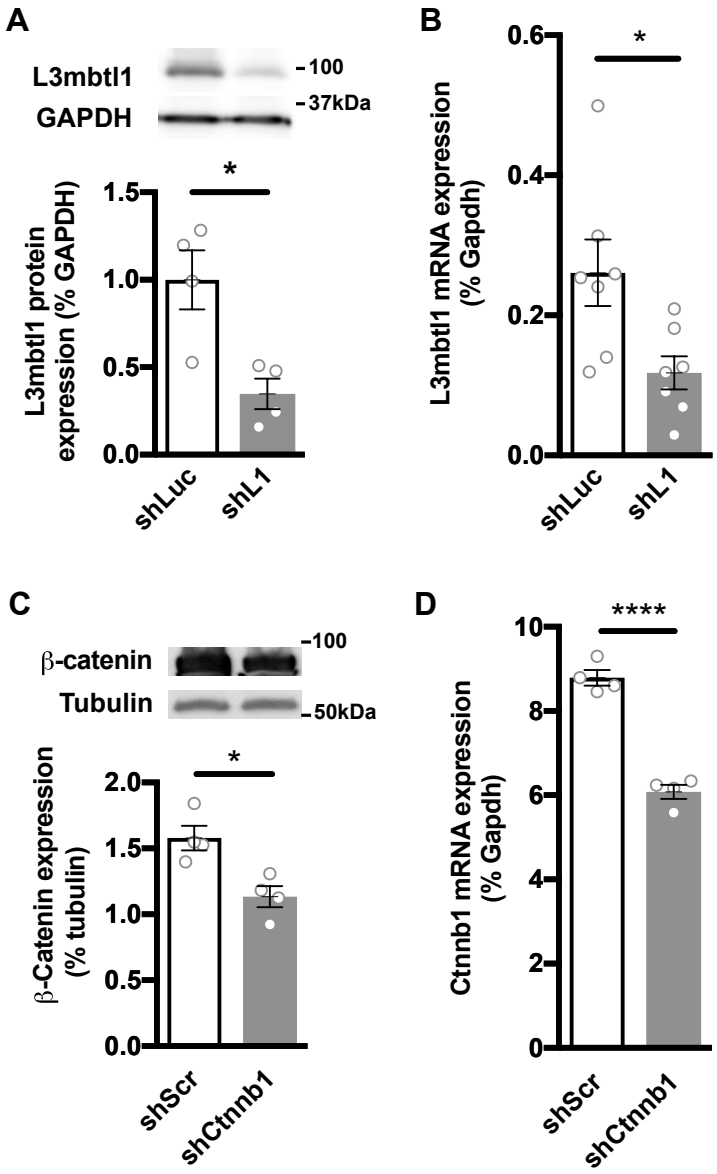

Figure S5. Validation of L3mbtl1 shRNA and Ctnnb1 shRNA. Related to Figure 4 and Figure 7. (A) Representative blots of L3mbtl1 (antibody #58) and GAPDH (top) and quantification (bottom) of exogenously expressed L3mbtl1 protein in HEK293T cells transfected with L3mbtl1 shRNA (shL1) or luciferase control shRNA (shLuc). *p=0.014, student's t-test, N = 4. **(B)** Endogenous L3mbtl1 mRNA levels in primary cultures expressing L3mbtl1 shRNA (shL1) or luciferase control shRNA (shLuc). Primary neurons were infected with high-titer lenti virus-packaged shRNAs for seven days. *p=0.019, student's t-test, N = 7. **(C)** Representative blots of Ctnnb1 and tubulin (top) and quantification (bottom) of exogenously expressed Ctnnb1 protein in HEK cells transfected with Ctnnb1 shRNA (shCtnnb1) or scramble control shRNA (shScr). *p=0.012, student's t-test, N = 4. **(D)** Endogenous Ctnnb1 mRNA levels in primary cultures expressing Ctnnb1 shRNA (shCtnnb1) or scramble control shRNA (shScr). Primary neurons were infected with high-titer lenti virus-packaged shRNAs for three days. ****p<0.0001, student's t-test. N = 4. Data shown are means ± SEM.

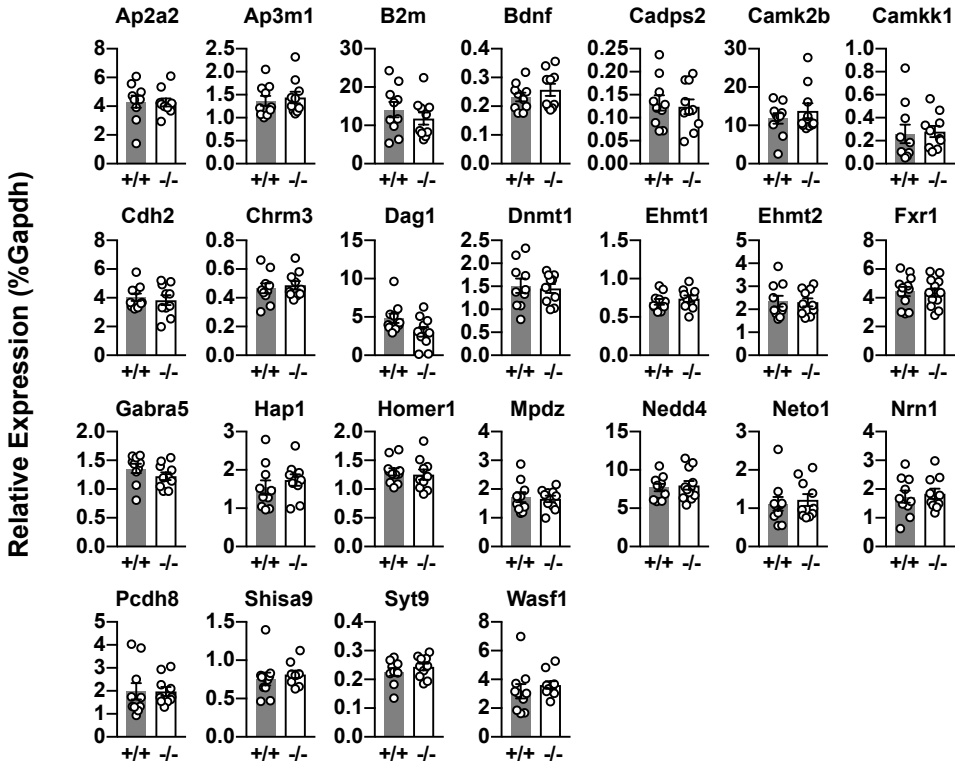

Figure S6. Identification of L3mbtl1 target genes. Related to Figure 6A. Quantification of RNA expression of candidate genes in Figure 6A by qPCR in hippocampal primary cultures from wild type and KO mice. Note that none of the genes were differentially regulated in L3mbtl1 KO neuronal cultures compared to wild type. Student's t-test, N = 8 - 12 independent cultures. Data shown are means ± SEM.

Best matched transcription factor	de novo sequence motif	% peaks with motif (% backgroud)	p-value
ETV5		76.97% (58.85%)	1E-147
E2F		68.10% (54.90%)	1E-74
BARHL2		44.61% (31.93%)	1E-71
NFkB-p65-Rel		44.37% (32.37%)	1E-64
Arnt:Ahr(bHLH)		66.02% (56.84%)	1E-36

Figure S7. Motif analysis for L3mbtl1-binding sites. Related to Figure 5. List of top enriched DNA-binding motifs identified by motif analysis performed on L3mbtl1 ChIP-seq peaks using HOMER de novo motif discovery.

SUPPLEMENTAL EXPERIMENTAL PROCEDURES

Expression and shRNA vectors

Full-length L3mbtl1 cDNA was PCR-amplified from mRNA isolated from hippocampal primary neurons and cloned in the pCAG vector. The shRNA vectors targeting L3mbtl1 and Ctnnb1 were purchased from Dharmacon (shL3mbtl1: #488433, shCtnnb1: #491202). The sequences of the control shRNA, scramble shRNA, is and 5´-ATCTCGCTTGGGCGAGAGTAAG-3´ (Dharmacon, #RHS4346). The β-catenin construct, mVenus-β-Catenin-20 (gift from Dr. Michael Davidson, Addgene #56604), was used for the validation of shRNA clones and overexpression in primary neurons.

Cell lines and transient transfection

HEK293T cells (American Type Culture Collection, MD, USA) were grown in Dulbecco's Modified Eagle's Medium (DMEM) supplemented with fetal bovine serum (10% v/v) and penicillin/streptomycin (100 units/ml), at 37 °C and in an atmosphere of 5% CO_2. Transfections were performed with Lipofectamine 2000 (Invitrogen). Cells were harvested 3 days after transfection.

Antibodies and Biochemistry

The N-terminal region of L3mbtl1 (aa 140-279, NP_001074807.1) was PCR-amplified and subcloned into pGEX-5X or -4T vector (glutathione *S*-transferase (GST) fusion protein, Amersham Pharmacia Biotech) to generate L3mbtl1 antibody. GST fusion proteins were purified using glutathione-Sepharose 4B resin (Amersham Pharmacia Biotech) and used to immunize rabbits. L3mbtl1 antibody #703 was affinity-purified using synthesized peptide (aa 140-169, Ac-RHEGGMARRDAGIQHPDVHQDRQDITSLEP-amide, AminoLink Coupling Gel, Pierce). L3mbtl1 antibody #58 was generated and purified by peptide aa 1-20 (Ac-MEGHTDMEILRTVKGSSTGE-amide). The following antibodies were also used: mouse anti-tubulin (dilution: 1:3000, Abcam); rabbit anti-β-catenin (1:10000, Abcam ab32572); mouse anti-Gapdh (1:2000, Millipore MAB374); HRP-conjugated anti-mouse and -rabbit IgG antibodies (GE Healthcare, 1:2000); normal rabbit IgG (CST, #2729); anti-GluA1 (Calbiochem #PC246, 1:200); anti-Vglut1 (synaptic systems #135304, 1:1000); anti-H3K4me3 (Abcam, ab8580); anti-H3K27ac (Abcam, ab4729).

RNA sequencing

Sequencing libraries were prepared according to ScriptSeq v2 protocol following rRNA depletion (RiboZero, Illumina), and run on single-end 50-bp modules in Illumina HiSeq 2000. Sequencing reads that passed the default purify filtering of Illumina CASAVA pipeline were quality trimmed/filtered using The FASTX-Toolkit (http://hannonlab.cshl.edu/fastx_toolkit) with a quality score cutoff of 20. Raw reads were first mapped to mouse GRCm38 genome using TopHat (v2.0.9) (Trapnell et al., 2009), then read counts were calculated for each replicate using HTSeq (v0.6.1) (Anders et al., 2015) with UCSC gene annotation. Differential gene expression analysis was carried out using DESeq2 (Love et al., 2014). A corrected $p<0.01$ and fold change >2.0 were applied to determine significant differences between treatment and control conditions (four biological replicates). Functional enrichment analysis was performed for all differentially expressed genes by DAVID6.8 (Huang da et al., 2009a, b). After clustering using default parameters, a representative category within each of the most significant clusters was selected. A heat map was generated by hierarchical clustering using ‘hclust’ and ‘heatmap.2’ function in R.

Chromatin Immunoprecipitation (ChIP)

Chromatin was prepared from P7-8 mouse hippocampal tissue and DIV14-16 hippocampal primary cultures. For each preparation, hippocampi or primary cultures from 18-22 mice were crosslinked by DSG, followed by the addition of formaldehyde to hippocampi and primary cultures. For ChIP against histone modifications, native histones were prepared from hippocampus without crosslinking. Nuclei preparation and chromatin digestion steps were done using a SimpleChIP Plus Enzymatic Chromatin IP Kit (Cell Signaling). Chromatin was digested to 100-500-bp fragments for ChIP-sequencing, or 300-1000-bp fragments for ChIP-qPCR. Immunoprecipitation procedures followed conventional procedures (Bharadwaj et al., 2013). MNase (micrococcal nuclease)-digested chromatin from wild type or L3mbtl1 KO mouse hippocampi and primary cultures was immunoprecipitated with 10μg anti-L3mbtl1 (#703), 2μg anti-H3K4me3 (Abcam, ab8580), 2μg anti-H3K27ac (Abcam, ab4729) or normal rabbit IgG as control.

After washing, chromatin complexes were eluted and the crosslinks were reversed. DNA was purified using MinElute columns (Qiagen). For qPCR reactions, 4% of immunoprecipitated DNA was used. Data are presented as the percentage of the unprecipitated (input) DNA or fold change over control sample.

ChIP sequencing and analysis

Libraries from three wild type samples and three L3mbtl1 KO samples were prepared from 10ng ChIP'd DNA each using a NEBNext Ultra DNA Library Prep Kit (NEB) and subjected to a 50bp single-end Illumina sequencing. Reads were aligned to the mm10/GRCm38 reference by Bowtie (v2.2.4) (Langmead et al., 2009). Peaks were called using the Irreproducible Discovery Rate (IDR) protocol (Li et al., 2011). In short, all three L3mbtl1 KO samples were pooled and used as control for peak callings. Peaks were called on individual wild type replicates, pooled wild type replicate, pseudoreplicates of individual wild type replicates, and pseudoreplicates of pooled wild type replicate. At least 100k peaks were called for each sample using MACS (v2.1.0) with a relaxed threshold: -p 0.05 --nomodel --extsize 165. IDR threshold of 0.01 and 0.0025 were used for self-consistency and pooled-consistency test respectively to determine the number of final peaks called. Peaks were annotated using HOMER (Heinz et al., 2010). Nearest genes were assigned to peaks within 1kb up- and down-stream from a TSS. Functional enrichment analysis was performed using DAVID6.8 (Huang da et al., 2009a, b). After clustering, a representative category within each of the most significant clusters was selected. For correlation analysis, peak chromosomal ranges generated from L3mbtl1 peaks above IDR threshold and those provided by GEO GSE63137 were mapped into windows of 10k nucleotides of mm10 genome, and pairwise Pearson correlation scores were plotted using R package corrplot v0.77. Read density distributions of ChIP-seq signals centered on the TSS +/- 3kb of each annotated transcript by the GRCm38.80.gtf were plotted using R package seqplots v1.12.0. Heatmaps were organized into 4 clusters based on K-means clustering of L3mbtl1 ChIP-seq signal patterns ("include" parameter). Average plots were plotted using log2 scaling. Motif analysis was performed using the Homer *de novo* motif discovery method.

***In situ* hybridization**

Fluorescein- or digoxigenin (DIG)-labeled cRNA probes were used for *in situ* hybridization: mouse L3mbtl1 (nucleotides 1289-2577; National Center for Biotechnology Information (NCBI) reference sequence NM_001081338.1), type 1 vesicular glutamate transporter (Vglut1; nucleotides 301–1680; GenBank accession number BC054462), 67 kDa glutamic acid decarboxylase (GAD67; nucleotides 1036–2015; NM_008077), glutamate/aspartate transporter (GLAST; nucleotides 1571–2473; AF330257), proteolipid protein (Plp; nucleotides 1-1359; NM_011123), and ionized calcium-binding adapter molecule 1 (Iba1; nucleotides 66-540; D86392). cRNA probes were synthesized as described previously (Yamasaki et al., 2010). Chromogenic or double-label fluorescent *in situ* hybridization was carried out as described (Kudo et al., 2012; Yamasaki et al., 2010). Briefly, tissues were prepared from mice at postnatal day 7 under isoflurane anesthesia. Brains were fixed by transcardial perfusion with 4% paraformaldehyde/0.1 M phosphate buffer (PB, pH7.2) for chromogenic *in situ* hybridization, or frozen on powdered dry ice for double-label fluorescent *in situ* hybridization. Brain slices (thickness 20 μm) were prepared with a cryostat (Leica VT1000S or CM3050S), and subjected successively to acetylation and prehybridization. Hybridization was carried out at 63.5°C with the hybridization buffer supplemented with cRNA probes diluted 1:1000. After stringent washing and blocking, immunohistochemical detection was performed. For chromogenic *in situ* hybridization, DIG-labeled cRNA probes were detected with alkaline phosphatase-conjugated anti-DIG antibody (1:500, Roche Diagnostic) and NBT/BCIP solution (1:50; Roche Diagnostics). Images were taken with a stereo microscope (SZX-7, Olympus) equipped with a CCD digital camera (INFINITY3-1UC, Lumenera). For double-label fluorescent *in situ* hybridization, fluorescein-labeled cRNA probes were visualized with peroxidase-conjugated anti-fluorescein antibody (1:500, Roche Diagnostics) and the TSA plus Fluorescein system (PerkinElmer). After inactivation of residual peroxidase activity introduced in the detection of fluorescein-labeled cRNA probes, DIG-labeled cRNA probes were detected with peroxidase-conjugated anti-DIG antibody (1:500, Roche Diagnostics) and the TSA plus Cy3 system (PerkinElmer). Nuclear staining was performed with DAPI (1:5000, Sigma). Images were acquired with a confocal laser scanning microscope (TCS SP5, Leica) equipped with a 20x oil immersion objective lens (HCX PL APO CS 20x/0.7 IMM). The specificity of cRNA probes against L3mbtl1 mRNA was confirmed by using L3mbtl1 KO mice. Other cRNA probes were validated by lack of hybridization signals with their sense probes. For quantification, the peak intensity for L3mbtl1 mRNA was measured in the soma of each cell type with ImageJ software. Background levels were determined as the mean peak intensity obtained from 80 excitatory neurons in L3mbtl1 KO mice (**Figure 1F**).

Immunocytochemistry and neuronal imaging

To identify spiny pyramidal neurons, cultured neurons were transfected with membrane-targeted farnesylated EGFP (EGFP-F) on DIV 11 using Lipofectamine 2000 (Invitrogen). For immunocytochemistry, neurons were fixed at DIV 14 with 4% paraformaldehyde (PFA)/4% sucrose for 10 min at room temperature, then blocked for 30 min in 0.1% bovine serum albumin (BSA), 4% normal goat serum, in PBS buffer pH 7.4. Surface staining of GluA1 was performed using an antibody against an extracellular epitope in the GluA1 N terminus, followed by Alexa Fluor-594 secondary antibody incubation in Triton-free buffer (1% BSA in PBS). Subsequently, neurons were permeabilized in PBST (0.1% Triton X-100), blocked again, incubated with anti-Vglut1 and anti-GFP primary antibody in Triton-containing buffer (1% BSA in PBST), followed with the corresponding Alexa Fluor-647 and Alexa Fluor-488 secondary antibodies. Images of 1024 x 1024 pixels were taken of hippocampal primary cultures using a confocal microscope (Zeiss LSM 700 with Axio Imager Z2) with a 63X objective (NA 1.4) and optical zoom of 1.0, with sequential acquisition settings. The z-stack images were taken at 0.35 μm depth intervals and pixel size 100 nm. For quantification, simultaneously cultured and stained sets of cells were imaged using identical settings. Measurements were performed in eight independent preparations and 4-6 cells per condition were analyzed for each preparation using ImageJ. Briefly, images were background subtracted, and a predetermined threshold was applied to each channel. Puncta were identified by unbiased ImageJ particle analysis. Colocalization was defined as any partially overlapping puncta. Neurons were analyzed for the total surface GluA1 integrated intensity and for the synaptic GluA1 (Vglut1-colocalized) integrated intensity per 20 μm dendritic length.

Lentiviral vector production and infection

Lentiviral particles were produced by co-transfecting HEK293T cells with a 3-plasmid system, including pGIPZ, psPAX2 packaging and pVSVG envelope vectors, as previously described (Lois et al., 2002; Naldini et al., 1996) with modifications. For knockdown experiments, primary neuron cultures were infected with virus particles for 3 days or 7 days. For L3mbtl1 knockdown experiments, infected cultures were selected using puromycin (3 μg/ml) for 48 hours.

Electrophysiology and data analysis

Thick-walled borosilicate glass pipettes were pulled to a resistance of 3–5 MΩ and filled with internal solution containing (in mM): 115 cesium methanesulfonate, 20 CsCl, 10 HEPES, 2.5 $MgCl_2$, 4 ATP disodium salt, 0.4 guanosine triphosphate trisodium salt, 10 sodium phosphocreatine, and 0.6 EGTA, at pH 7.25, with CsOH. The extracellular solution consisted of (in mM) 119 NaCl, 2.5 KCl, 4 $CaCl_2$, 4 $MgCl_2$, 26 $NaHCO_3$, 1 NaH_2PO4, and 11 glucose, gassed with 5% CO_2 and 95% O_2, pH of 7.4, unless otherwise noted. AMPAR-mediated miniature EPSCs were measured with whole-cell voltage-clamp in the presence of picrotoxin (0.1 mM, Sigma) with or without tetrodotoxin (TTX, 0.001 mM, Ascent Scientific), respectively. For recordings of spontaneous spiking, current-clamp recordings were performed. Potassium-based internal solution was used. NBQX (0.005 mM, Ascent Scientific), PTX (0.1 mM, Sigma), and/or D-APV (0.05 mM, Ascent Scientific) were added to the extracellular solution. For recordings of $GABA_AR$-mediated miniature IPSCs, cesium-based internal solution was used and recordings were performed in the extracellular solution containing NBQX, DL-APV and TTX. All experiments and analyses of data were performed in a blind manner. Recordings were performed using a MultiClamp 700B amplifier and Digidata 1440, and digitized at 10 kHz and filtered at 4 kHz by low-pass filter. Data were acquired and analyzed using pClamp (Molecular Devices) and Mini Analysis software (Synaptosoft). For mini analysis, approximately three hundred events were sampled from each experiment and events smaller than 5 pA were excluded. To test for multiplicative scaling of mini amplitude distributions, we followed a previously described method (Kim et al., 2012). To ensure that each group had an equal number of events and each cell contributes equally to the group, we randomly picked an equal number of events per cell to make up a total number of 2000 events for each group. Briefly, we scaled down values from the group with larger amplitude ("treat") to the group with smaller amplitude ("control"), by multiplying an arbitrary scaling factor (between 0 and 1), and then excluded any amplitudes that fell below the threshold. The threshold is determined by the smallest amplitude of the "control" group. The degrees of overlap between scaled "treat" and "control" data were assessed with various scaling factors, and the largest p value obtained from the Kolmogorov Smirnov (KS) test was reported for each experiments.

Primers and probes

For RNA expression analysis, the following TaqMan gene expression assays (Applied Biosystems) were used:

Taqman gene expression assay

Gene	Catalog #	Gene	Catalog #
Ap2a2	Mm01279159_m1	Gabra2	Mm00433435_m1
Bdnf	Mm04230607_s1	Gabra5	Mm00621092_m1
Camk2b	Mm00432284_m1	Gapdh	Mm99999915_g1
Camkk1	Mm00517053_m1	Homer1	Mm00516275_m1
Cdh2	Mm01162497_m1	Itgb1	Mm01253230_m1
Cfl1	Mm03057591_g1	L3mbtl1	Mm01239967_m1
Ctnnb1	Mm00483039_m1	Nedd4	Mm00456829_m1
Cxcr4	Mm01996749_s1	Shank3	Mm00498775_m1
Dag1	Mm00802400_m1	Ywhaz	Mm03950126_s1
Fxr1	Mm00484523_m1		

For ChIP-qPCR, the following EpiTect ChIP qPCR assays (Qiagen) were used:

Epitect ChIP qPCR Primers

Gene	Catalog #
Ctnnb1	GPM1041109(-)01A
Gabra2	GPM1051280(-)01A
Igx1a (intergenic)	GPM100001C(-)01A

SUPPLEMENTAL REFERENCES

Anders, S., Pyl, P.T., and Huber, W. (2015). HTSeq--a Python framework to work with high-throughput sequencing data. Bioinformatics 31, 166-169.

Bharadwaj, R., Jiang, Y., Mao, W., Jakovcevski, M., Dincer, A., Krueger, W., Garbett, K., Whittle, C., Tushir, J.S., Liu, J., *et al.* (2013). Conserved chromosome 2q31 conformations are associated with transcriptional regulation of GAD1 GABA synthesis enzyme and altered in prefrontal cortex of subjects with schizophrenia. J Neurosci 33, 11839-11851.

Heinz, S., Benner, C., Spann, N., Bertolino, E., Lin, Y.C., Laslo, P., Cheng, J.X., Murre, C., Singh, H., and Glass, C.K. (2010). Simple combinations of lineage-determining transcription factors prime cis-regulatory elements required for macrophage and B cell identities. Mol Cell 38, 576-589.

Huang da, W., Sherman, B.T., and Lempicki, R.A. (2009a). Bioinformatics enrichment tools: paths toward the comprehensive functional analysis of large gene lists. Nucleic acids research 37, 1-13.

Huang da, W., Sherman, B.T., and Lempicki, R.A. (2009b). Systematic and integrative analysis of large gene lists using DAVID bioinformatics resources. Nat Protoc 4, 44-57.

Kudo, T., Uchigashima, M., Miyazaki, T., Konno, K., Yamasaki, M., Yanagawa, Y., Minami, M., and Watanabe, M. (2012). Three types of neurochemical projection from the bed nucleus of the stria terminalis to the ventral tegmental area in adult mice. J Neurosci 32, 18035-18046.

Langmead, B., Trapnell, C., Pop, M., and Salzberg, S.L. (2009). Ultrafast and memory-efficient alignment of short DNA sequences to the human genome. Genome biology 10, R25.

Li, Q., Brown, J.B., Huang, H., and Bickel, P.J. (2011). Measuring reproducibility of high-throughput experiments. Ann Appl Stat 5, 1752-1779.

Lois, C., Hong, E.J., Pease, S., Brown, E.J., and Baltimore, D. (2002). Germline transmission and tissue-specific expression of transgenes delivered by lentiviral vectors. Science 295, 868-872.

Love, M.I., Huber, W., and Anders, S. (2014). Moderated estimation of fold change and dispersion for RNA-seq data with DESeq2. Genome biology 15, 550.

Naldini, L., Blomer, U., Gallay, P., Ory, D., Mulligan, R., Gage, F.H., Verma, I.M., and Trono, D. (1996). In vivo gene delivery and stable transduction of nondividing cells by a lentiviral vector. Science 272, 263-267.

Trapnell, C., Pachter, L., and Salzberg, S.L. (2009). TopHat: discovering splice junctions with RNA-Seq. Bioinformatics 25, 1105-1111.

Yamasaki, M., Matsui, M., and Watanabe, M. (2010). Preferential localization of muscarinic M1 receptor on dendritic shaft and spine of cortical pyramidal cells and its anatomical evidence for volume transmission. J Neurosci 30, 4408-4418.